

PACS numbers: 71.15.Ap, 71.15.Dx, 71.15.Mb, 71.20.Nr

**ELECTRONIC PROPERTIES OF TIN TELLURIDE:
A FIRST PRINCIPLES STUDY**

G. Sharma¹, P. Bhambhani¹, N. Munjal¹, V. Sharma², B.K. Sharma³

¹ Department of Physics, Banasthali University,
Banasthali, 304022, India
E-mail: gsphysics@gmail.com

² School of Physics and DST/NRF Centre of Excellence in Strong Materials,
University of the Witwatersrand,
Johannesburg, 2050 South Africa

³ Department of Physics, University of Rajasthan,
Jaipur, 302005, India

In this paper, using the linear combination of atomic orbitals (LCAO) method, the electronic structure and ground state properties of the IV-VI semiconductor, SnTe are reported. To study the electron momentum density, autocorrelation function, the ab initio calculations are performed within the exchange scheme of Becke and the correlation energy functional of Perdew-Burke-Ernzerhof (PBE). The calculated Compton profiles are used to discuss the electronic properties of the SnTe. On the basis of equal-valence-electron-density profiles and valence-electron charge-density maps, we examined the nature of bonding in this compound. Our study suggests that SnTe shows more ionicity in comparison to GeTe, which is found to be in agreement with earlier data.

Keywords: SNTE, ELECTRON MOMENTUM DENSITY, IV-VI SEMICONDUCTOR, LCAO METHOD.

(Received 04 February 2011, in final form 29 April 2011)

1. INTRODUCTION

The IV-VI semiconductor compounds, in particular which crystallize in rocksalt-structure, have been of great interest due to the fascinating properties like, have small band gaps, high dielectric constants, and a variety of very unusual thermodynamic, vibration, electronic, and infrared properties [1, 2]. In these IV-VI semiconductors Tin telluride, SnTe, is important in several practical applications such as SnTe and its alloys are well known for their use as infrared detectors, infrared lasers, micro electronic and thermo electric devices [3, 4]. SnTe which has NaCl type (B1) cubic structure ($O_h^5 = Fm\bar{3}m$) undergoes structural transformation to orthorhombic structure ($D_{2h}^{16} = P_{nma}$) under pressure [5, 6].

For SnTe, although number of studies on electronic, optical and structural properties has been reported in earlier work [5-13], but the electronic properties like electron momentum density, autocorrelation function and bonding through Compton profile are rarely attempted. Therefore, the aim of the present work is to study the electronic structure of SnTe through the Compton profile calculated from the first-principles technique.

In this paper, we report the electronic properties such as electron momentum density, autocorrelation function and bonding in SnTe using LCAO method based on the density functional theory (DFT). In this paper, unless stated, all quantities are in atomic units (a.u.) where $e = \hbar = m = 1$ and $c = 137.036$, giving unit momentum = 1.9929×10^{-24} kg·m·s⁻¹, unit energy = 27.212 eV and unit length = 5.2918×10^{-11} m.

2. COMPUTATIONAL DETAILS

The CRYSTAL code [14] provides a platform to calculate electronic structure of periodic systems with Gaussian basis employing the *ab-initio* LCAO method. A few fundamental schemes exist to construct Hamiltonian for the periodic solids, in which Hartree-Fock (HF) approximation and the density functional theory (DFT) are the well known approaches among these schemes. There are a number of functionals existing in literature to treat exchange and correlation under the DFT. In the present calculations, the local functions were constructed from the Gaussian type basis sets [15] and the Kohn-Sham Hamiltonian was constructed while considering the exchange scheme of Becke [16] and PBE correlation scheme [17]. The calculations were performed for B1 structure (space group $Fm\bar{3}m$) with a lattice constant $a = 6.237$ Å for the compound. The self-consistent calculations were performed considering $29\bar{k}$ points in the irreducible Brillouin zone.

Compton profile is derived from the ground state electron momentum density distribution in solids. In the independent particle model the momentum density $n(p)$ is given by [18, 19]:

$$n(p) \propto \sum_i \left| \int \psi_i(\mathbf{r}) \exp(-i\mathbf{p}\cdot\mathbf{r}) d\mathbf{r} \right|^2 \quad (1)$$

where $n(p)$ is the three dimensional momentum distribution and $\psi(\mathbf{r})$ represents the electron wave function. The summation is all over the occupied states. The Compton profile can be derived from the ground state momentum density $n(p)$ as:

$$J(p_z) = \int_{-\infty}^{+\infty} \int_{-\infty}^{+\infty} n(p) dp_x dp_y \quad (2)$$

The Compton profiles were calculated over the range of 0-10 a.u to count 9.8715 electrons in the compound.

3. RESULTS AND DISCUSSION

As stated earlier, we have computed Compton profiles of SnTe from the DFT-LCAO method. In Table 1, the numerical values of the unconvoluted theoretical Compton profiles along the principal crystallographic directions, namely, [100], [110] and [111] together with the average Compton profile derived from the DFT-LCAO method are given. To study the anisotropy in the theoretical momentum densities, in Fig. 1 we have plotted the directional difference curves viz. [100]-[110], [100]-[111] and [110]-[111]. It is evident from Fig. 1 that all anisotropies are positive in nature and also the anisotropy

between [100] and [111] directions is maximum around $p_z = 0$ a.u. In Fig. 1, the maximum anisotropy (0.26 e/a.u. i.e. 4.94% of $J_{ave}(0)$) is seen between [100]-[110] directions at $p_z = 0.7$ a.u. Figure 1 also reveals that the anisotropy [110]-[111] is small in magnitude in the entire range of momentum as compared to other two anisotropies and the anisotropies are hardly visible beyond 3.0 a.u as the reason is mainly contributed by the core electrons which remain almost unaffected during the solid formation. Moreover, measurements along the principal directions of SnTe would be valuable to test these predictions and hence examine the relative performance of various schemes of computation and anisotropies.

The Compton profiles can also be analyzed in real space by taking their Fourier transforms. The real space transform of the momentum density, and thereby the Compton profile data, is normally known as autocorrelation function (AF) or the reciprocal form factor $B(z)$. This function is directly

Table 1 – Unconvoluted valence Compton profiles of SnTe computed using PBE correlation functional within the DFT–LCAO method

p_z (a.u.)	$J(p_z)$ in e/a.u.			
	J_{100}	J_{110}	J_{111}	J_{ave}
0.0	5.3648	5.2789	5.2060	5.2595
0.1	5.2703	5.2134	5.1582	5.2196
0.2	5.0298	5.0437	5.0182	5.0973
0.3	4.7360	4.8133	4.7920	4.8858
0.4	4.4527	4.5227	4.4825	4.5772
0.5	4.1643	4.1297	4.0901	4.1675
0.6	3.7973	3.6134	3.6216	3.6653
0.7	3.2915	3.0228	3.0991	3.1002
0.8	2.6623	2.4520	2.5608	2.5217
1.0	1.4278	1.5872	1.6035	1.5363
1.2	0.7607	0.9990	0.9609	0.9355
1.4	0.5556	0.6191	0.6246	0.6336
1.6	0.4959	0.4858	0.4911	0.5027
1.8	0.5059	0.4543	0.4471	0.4569
2.0	0.4894	0.4136	0.4123	0.4195
3.0	0.1455	0.1392	0.1392	0.1367
4.0	0.0496	0.0483	0.0479	0.0449
5.0	0.0387	0.0383	0.0381	0.0346
6.0	0.0264	0.0265	0.0266	0.0227
7.0	0.0140	0.0143	0.0143	0.0103
8.0	0.0073	0.0075	0.0076	0.0035
9.0	0.0048	0.0049	0.0050	0.0009
10.0	0.0040	0.0040	0.0041	0.0001

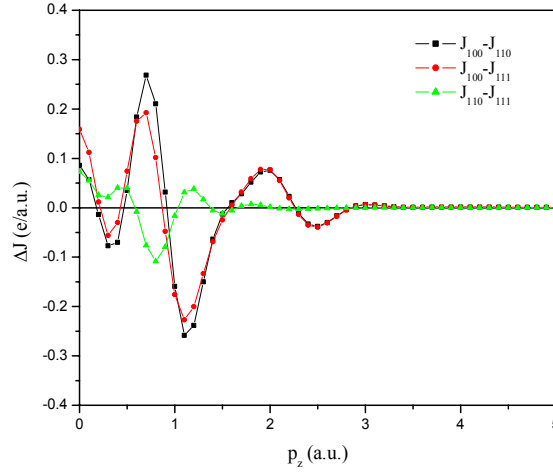


Fig. 1 – Compton profile anisotropies, using PBE correlation functional, obtained from unconvoluted directional Compton profiles for SnTe

associated with the formation of bonds and facilitates the identification of bonding in solids [19-21]. The resulting function known as autocorrelation function can be written as,

$$B(z) = \int_{-\infty}^{+\infty} J(p_z) \exp(ip_z z) dp_z \quad (3)$$

In the present study, we have calculated the momentum density up to 10 a.u., which is found to be sufficient to count the total valence electrons in the compound. The transform mentioned in Eqⁿ. 3 is used to determine the autocorrelation function and shown in Fig. 2. It is worthwhile to mention here that at the position of minimum occurrence, there is a large overlap between the functions indicating covalent nature of bonding. The dip which relates this overlapping is clearly visible at 4.4 a.u. indicates the covalent nature of bonding in SnTe. As the $B(z)$ function plotted, is derived from the spherical average of the directional profile only the gross features are visible. Therefore, it would be interesting to perform Compton profile measurements on single crystalline samples of SnTe to obtain $B(z)$ functions.

For a more relevant discussion, we have compared the nature of bonding in SnTe with other isoelectronic IV-VI compound i.e. GeTe. As mentioned earlier, above the transition temperature, SnTe crystallizes in the rocksalt (NaCl) structure. GeTe, on the other hand, is face centred rhombic; however, the distortion from fcc is small, and we have assumed, as is usually the case, the rocksalt structure also. In Fig. 3, we have plotted the equal valence electron density (EVED) profiles deduced from DFT-LCAO valence values. The difference between two EVED profiles is also shown in the inset. The EVED profiles were derived by normalizing valence electron profiles to 5.0 electrons and scaling the resulting profiles by the Fermi momentum (p_F). For SnTe and GeTe, p_F turned out to be 0.8846 and 0.9334 a.u. respectively using the expression $(3\pi^2 n)^{1/3}$ where n is the valence electron density. According to Reed and Eisenberger [22], this scheme offers a way to

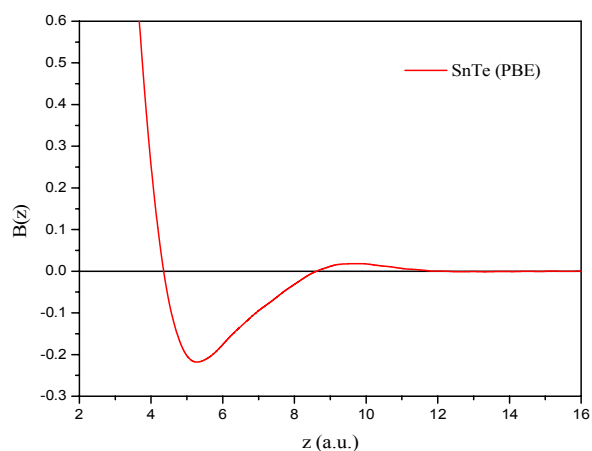


Fig. 2 – The autocorrelation function $B(z)$ derived from the DFT-PBE and the free atom valence profile of SnTe. Here z is the direction of scattering vector and theoretical valence profile is not attenuated

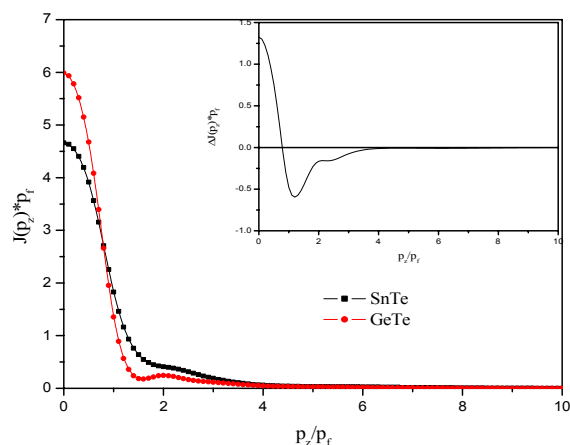


Fig. 3 – The equal-valence-electron-density (EVED) profiles, deduced from the unconvoluted theoretical valence profiles, of SnTe and GeTe ($p_F = 0.884$ and 0.933 a.u. respectively). In the inset difference between EVED profiles is also shown. Both profiles are normalized to 5.0 electrons

understand the nature of bonding, to a first approximation, in isoelectronic compounds. Fig. 3 reveals that the EVED profile corresponding to GeTe is larger around the low momentum region as compared to SnTe. As larger value around low momentum is attributed to larger covalent character, it points that SnTe is less covalent and more ionic than GeTe. The larger ionicity of SnTe compared to GeTe is well supported by the results of Shalvoy et al. [23]. The trend of ionicity can also be explained on the basis of two-dimensional valence charge density (VCD) of SnTe and GeTe. In Fig. 4, the VCD maps for SnTe and GeTe are plotted. It is seen that the charge densities in both tellurides are quite different and large amount of bond

charge is seen between Ge and Te in the interstitial region of GeTe, which reconfirms more covalent character of GeTe in comparison to SnTe.

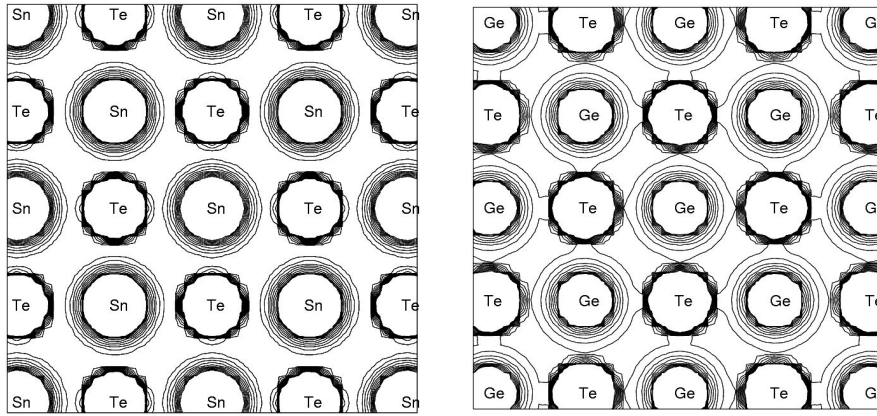


Fig. 4 – Valence-electron charge density of SnTe and GeTe computed using DFT-LCAO method

CONCLUSIONS

In this paper, the electronic properties of SnTe are presented. The theoretical anisotropies [100]-[110], [100]-[111] and [110]-[111] are derived using the DFT-LCAO method for the compound. The anisotropies in directional Compton profiles obtained from LCAO calculation indicate the maximum anisotropy i.e. 4.94 % of J_{ave} between [100] and [110] directions at $p_z = 0.7$ a.u. On the basis of EVED profiles and valence-electron charge-density maps it is found that SnTe is less covalent and more ionic than GeTe. Directional measurements are needed to examine the anisotropies and analyze the performance of various schemes of computation and the occupied states.

This work is financially supported by the University Grant Commission (UGC) through Emeritus Fellowship and SR/33-37/2007 to BKS. The financial support provided by DST, New Delhi for the project “Banasthali Centre for Education and Research in Basic Sciences” under their CURIE programme is gratefully acknowledged. VS acknowledge the support from the DST/NRF Centre of Excellence in strong materials, University of Witwatersrand, Johannesburg, South Africa.

REFERENCES

1. P.K. Nair, M. Ocampo, A. Fernandez, M.T.S. Nair, *Solar Energy Mater.* **20**, 235, (1990).
2. L.D. Hicks, T.C. Harman, X. Sun, M.S. Dresselhaus, *Phys. Rev. B* **53**, R10493 (1996).
3. T.K. Chaudhuri, *Int. J. Energy Res.* **16**, 481 (1992).
4. G.P. Agrawal, N.K. Dutta, *Semiconductor Lasers* (New York: Van Nostrand-Reinhold:1993).
5. T. Chattopadhyay, H.G. Von Schnering, W.A. Groshans, W.B. Holzapfel, *Physica B* **139/140**, 356 (1986).

6. P.B. Littlewood, B. Mihaila, R.K. Schulze, D.J. Safarik, J.E. Gubernatis, A. Bostwick, E. Rotenberg, C.P. Opeil, T. Durakiewicz, J.L. Smith, J.C. Lashley, *Phys. Rev. Lett.* **105**, 086404 (2010).
7. N.S. Dantas, A.F. da Silva, C. Persson, *Opt. Mat.* **30**, 1451 (2008).
8. N.E. Zein, V.I. Zinenko, A.S. Fedorov, *Phys. Lett. A* **164**, 115 (1992).
9. S. Aripionammal, C. Venkateswaran, S. Natarajan, *phys. stat. sol. B* **197**, K1 (1996).
10. K. Hoang, S.D. Mahanti, M.G. Kanatzidis, *Phys. Rev. B* **81**, 115106 (2010).
11. X. Gao, M.S. Daw, *Phys. Rev. B* **77**, 033103 (2008).
12. C.M.I. Okoye, *J. Phys.: Condens. Matter* **14**, 8625 (2002).
13. A.A. Volykhov, V.I. Shtanov, L.V. Yashina, *Inorg. Mater.* **44**, 345 (2008).
14. R. Dovesi, V.R. Saunders, C. Roetti, R. Orlando, C.M. Zicovich-Wilson, F. Pascale, B. Civalleri, K. Doll, N.M. Harrison, I.J. Bush, Ph. D'Arco and M. Llunell, CRYSTAL06 User's manual, University of Torino, Torino, 2006.
15. <http://www.crystal.unito.it>
16. D. Becke, *J. Chem. Phys.* **98**, 5648 (1993).
17. J.P. Perdew, K. Burke, M. Ernzerhof, *Phys. Rev. Lett.* **77**, 3865 (1996), **78**, 1396(E) (1997).
18. B.G. Williams, *Compton scattering* (New York, McGraw-Hill: 1977).
19. M.J. Cooper, P.E. Mijnarends, N. Shiotani, N. Sakai, A. Bansil, *X-ray Compton Scattering* (Oxford University Press; 2004).
20. W. Weyrich, P. Pattison, B. Williams, *Chem. Phys.* **41**, 271 (1979).
21. P. Pattison, N.K. Hansen, J.R. Schneider, *Chem. Phys.* **59**, 231 (1981).
22. W.A. Reed, P. Eisenberger, *Phys. Rev. B* **6**, 4596 (1972).
23. R.B. Shalvoy, G.B. Fisher, P.J. Stiles, *Phys. Rev. B* **15**, 1680 (1977).